Marangoni Effects on Evaporative Lithographic Patterning of Colloidal Films

Daniel J. Harris and Jennifer A. Lewis*

Frederick Seitz Materials Research Laboratory and Materials Science and Engineering Department, University of Illinois, Urbana, Illinois 61801

Received January 8, 2008. In Final Form: February 12, 2008

We investigate the effects of Marangoni stresses on the evaporative lithographic patterning of colloidal films (Harris, D. J.; Hu, H.; Conrad, J. C.; Lewis, J. A. *Phys. Rev. Lett.* **2007**, *98* (14), 148301). Films are dried beneath a mask that induces periodically varying regions of free and hindered evaporation. Direct imaging reveals that silica microspheres suspended within an organic solvent exhibit recirculating flows induced by temperature and surface tension gradients that arise during drying. The films display remarkable pattern formation with a majority of the particles deposited in the masked regions. Above a critical colloid volume fraction, recirculating flows are suppressed, leading to particle deposition in unmasked regions of high evaporative flux.

The ability to pattern colloidal films is of growing importance for novel coatings,[2,3] metallized ceramic layers,[4] and even high throughput DNA screening.[5] Most patterning approaches guide colloidal assembly either through chemical[6−8] or topographical[9−12] modification of the underlying substrate or by application of an external field.[13−18] However, these approaches typically require multiple processing steps and are often limited to only a few particle layers. To overcome such limitations, we recently pioneered a new route for patterning colloidal films, known as evaporative lithography.[1]

Our approach builds on prior observations of fluid flow and particle migration in freely evaporating aqueous[19−26] and organic[27−32] droplets. In aqueous colloidal droplets (or films), contact line pinning and higher evaporation rates at the edge of the drop lead to the outward flow of fluid and entrained particles, yielding the well-known "coffee-ring" pattern.[19] By contrast, the outward flow of fluid and entrained particles is reversed in freely evaporating drops composed of nonaqueous colloidal suspensions due to Marangoni stresses.[28] Evaporative cooling and inefficient heat transfer through the drop induces a temperature gradient, which in turn leads to a gradient in surface tension across the drop's surface such that the temperature is lowest and the surface tension is highest at the center of the drop. Recirculating flows develop as fluid is transported from regions of lowest surface tension to regions of highest surface tension. Unlike aqueous colloidal films, a majority of the particles are now deposited in the center of the drop rather than at its edge.

In this letter, we investigate the effects of Marangoni stresses on the evaporative lithographic patterning of nonaqueous colloidal films. A schematic of this patterning approach is provided in Figure 1. Films are dried beneath a mask that induces periodic variations between free and hindered evaporation that give rise to periodic temperature (and surface tension) gradients across the film surface, in which cooler regions develop beneath the open features (holes) within the mask. We directly image the induced recirculating flows within films composed of fluorescent-core silica microspheres suspended in ethanol and dried under a patterned mask. We further demonstrate that particles are deposited at the interfaces that develop between hexagonal recirculating flow cells, resulting in inverse pattern formation upon drying a dilute colloidal film. Above a critical initial volume fraction ($\phi_c \sim 0.22$), these recirculating flows cease and particles are now deposited in regions of highest evaporative flux, that is, beneath the open features. A broad range of patterned colloidal

* To whom correspondence should be addressed. E-mail: jalewis@uiuc.edu.

(1) Harris, D. J.; Hu, H.; Conrad, J. C.; Lewis, J. A. *Phys. Rev. Lett.* **2007**, *98* (14), 148301.
(2) Sun, J.; Gerberich, W. W.; Francis, L. F. *J. Polym. Sci., Part B: Polym. Phys.* **2003**, *41* (14), 1744−1761.
(3) Martinez, C. J.; Lewis, J. A. *Langmuir* **2002**, *18* (12), 4689−4698.
(4) Masuda, Y.; Koumura, T.; Okawa, T.; Koumoto, K. *J. Colloid Interface Sci.* **2003**, *263* (1), 190−195.
(5) Jing, J.; Reed, J.; Huang, J.; Hu, X.; Clarke, V.; Edington, J.; Housman, D.; Anantharaman, T. S.; Huff, E. J.; Mishra, B.; Porter, B.; Shenker, A.; Wolfson, E.; Hoirt, C.; Kantor, R.; Aston, C.; Schwartz, D. C. *Proc. Natl. Acad. Sci. U.S.A.* **1998**, *95*, 8046−8051.
(6) Aizenberg, J.; Braun, P. V.; Wiltzius, P. *Phys. Rev. Lett.* **2000**, *84* (13), 2997−3000.
(7) Zheng, H.; Lee, I.; Rubner, M. F.; Hammond, P. T. *Adv. Mater.* **2002**, *14* (8), 569−572.
(8) Lee, I.; Zheng, H.; Rubner, M. F.; Hammond, P. T. *Adv. Mater.* **2002**, *14* (8), 572−577.
(9) Lee, W.; Chan, A. T.; Bevan, M. A.; Lewis, J. A.; Braun, P. V. *Langmuir* **2004**, *20* (13), 5262−5270.
(10) Van Blaaderen, A.; Ruel, R.; Wiltzius, P. *Nature* **1997**, *385*, 321−324.
(11) Yin, Y.; Lu, Y.; Gates, B.; Xia, Y. *J. Am. Chem. Soc.* **2001**, *123* (36), 8718−8729.
(12) Lin, K. H.; Crocker, J. C.; Prasad, V.; Schofield, A.; Weitz, D. A.; Lubensky, T. C.; Yodh, A. G. *Phys. Rev. Lett.* **2000**, *85* (8), 1770−1773.
(13) Richetti, P.; Prost, J.; Barois, P. *J. Phys. Lett.* **1984**, *45* (23), 1137−1143.
(14) Hayward, R. C.; Saville, D. A.; Aksay, I. A. *Nature* **2000**, *404* (6773), 56−59.
(15) Ristenpart, W. D.; Aksay, I. A.; Saville, D. A. *Phys. Rev. Lett.* **2003**, *90* (12), 128303.
(16) Ristenpart, W. D.; Aksay, I. A.; Saville, D. A. *Phys. Rev. E* **2004**, *69* (2), 021405.
(17) Bhatt, K. H.; Grego, S.; Velev, O. D. *Langmuir* **2005**, *21* (14), 6603−6612.
(18) Velev, O. D.; Bhatt, K. H. *Soft Matter* **2006**, *2* (9), 738−750.
(19) Deegan, R. D.; Bakajin, O.; Dupont, T. F.; Huber, G.; Nagel, S. R.; Witten, T. A. *Nature* **1997**, *389* (6653), 827−829.
(20) Deegan, R. D.; Bakajin, O.; Dupont, T. F.; Huber, G.; Nagel, S. R.; Witten, T. A. *Phys. Rev. E* **2000**, *62* (1), 756−765.
(21) Deegan, R. D. *Phys. Rev. E* **2000**, *61* (1), 475−485.
(22) Routh, A. F.; Russel, W. B. *AIChE J.* **1998**, *44* (9), 2088−2098.
(23) Smalyukh, I. I.; Zribi, O. V.; Butler, J. C.; Lavrentovich, O. D.; Wong, G. C. L. *Phys. Rev. Lett.* **2006**, *96* (17), 177801.
(24) Shmuylovich, L.; Shen, A. Q.; Stone, H. A. *Langmuir* **2002**, *18* (9), 3441−3445.
(25) Chiu, R. C.; Cima, M. J. *J. Am. Ceram. Soc.* **1993**, *76* (11), 2769−2777.
(26) Hu, H.; Larson, R. G. *Langmuir* **2005**, *21* (9), 3963−3971.
(27) Hu, H.; Larson, R. G. *Langmuir* **2005**, *21* (9), 3972−3980.
(28) Hu, H.; Larson, R. G. *J. Phys. Chem. B* **2006**, *110* (14), 7090−7094.
(29) Savino, R.; Paterna, D.; Favaloro, N. *J. Thermophys. Heat Transfer* **2002**, *16* (4), 562−574.
(30) Berg, J. C.; Boudart, M.; Acrivos, A. *J. Fluid Mech.* **1966**, *24*, 721−735.
(31) Girard, F.; Antoni, M.; Faure, S.; Steinchen, A. *Langmuir* **2006**, *22* (26), 11085−11091.
(32) Ristenpart, W. D.; Kim, P. G.; Domingues, C.; Wan, J.; Stone, H. A. *Phys. Rev. Lett.* **2007**, *99* (23), 234502.

10.1021/la8000637 CCC: $40.75
Published on Web 03/04/2008 PAGE EST: 3.8

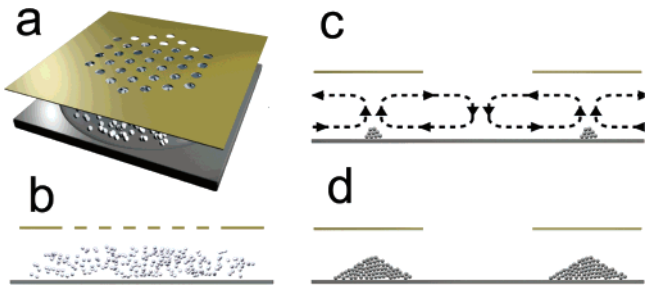

Figure 1. Schematic presentation of the evaporative lithography process, which shows the (a) top view of the mask design and (b) side view of an as-deposited film along with magnified (side) views of the (c) recirculating flow cells and (d) particle deposition in the patterned film.

films can be generated simply by tuning the initial colloid volume fraction and mask design.

Colloidal films are produced from silica microspheres of radius $a = 473 \pm 6$ nm (Fuso Chemical Co., LTD, Japan) suspended in ethanol, unless otherwise noted. A monolayer of 3-(trimethoxysilyl)propyl methacrylate (TPM; Sigma-Aldrich, Inc.) is grafted onto the surface of the microspheres, following the procedure outlined in ref 33, to provide stabilization in nonaqueous media. Tracer particles composed of fluorescent-core silica microspheres ($a = 492 \pm 58$ nm) are synthesized with rhodamine isothiocyanate (RITC; Sigma-Aldrich, Inc.)[34,35] to aid flow visualization and coated with TPM. Colloidal suspensions are prepared with varying initial microsphere volume fractions, ϕ_i, ranging from 0.001 to 0.15. Films are prepared by depositing an appropriate amount of a given suspension onto a glass substrate to achieve an initial film height, $h_i \approx 100\ \mu$m, followed by drying under a patterned mask. Multiple mask designs are utilized in this study. One set contains a hexagonal array of holes of diameter $d_h = 250$ or 500 μm and center-to-center hole spacing, or pitch, P, of $2d_h$ or $5d_h$. Another design consists of an array of parallel lines with thickness $d_l = 200\ \mu$m and $P = 5d_l$. Each mask is supported above the drying film by a thin section of brass shim stock to ensure a separation distance between the mask and underlying film, or gap height, h_g, of nominally 30 μm.

To directly observe Marangoni effects on particle migration during evaporative lithography, we use fluorescence microscopy to image the flow of fluorescently labeled silica microspheres. Particle flow is observed on a fast camera (Phantom V7.1, Vision Research) attached to an inverted microscope (IX71, Olympus). We fix $\phi_i = 0.001$ and acquire image sequences of a series of films drying under masks with $d_h = 250$, $P = 2d_h$ or $5d_h$ and $h_g \approx 30\ \mu$m (Figure 2). The focal plane in the acquired images resides slightly above the substrate surface. Hexagonal recirculating flow cells develop almost instantaneously when the mask is placed above the drying film. They are partitioned such that each hexagonal cell is centered below an open feature (or hole) within the mask, while the interfaces between these cells reside beneath the masked area surrounding each feature (Figure 2a). As drying proceeds, a dark region emerges in the middle of each cell that is devoid of particles (Figure 2a−c). The size of this depleted region grows upon further evaporation, and the particles remain confined within the bright border regions that exhibit recirculating flows (Figure 2d). Upon further evaporation, the particles continue to reside in the nonevaporating regions and are ultimately deposited onto the substrate in a pattern that is the negative of the drying mask.

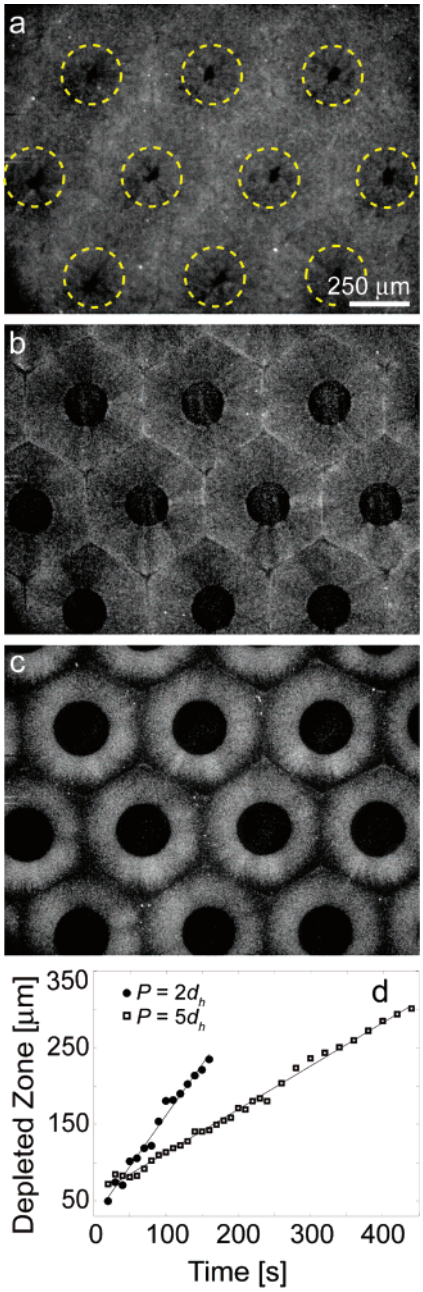

Figure 2. Fluorescence images of a colloidal film prepared at $\phi_i = 0.001$ and dried under a mask with $d_h = 250\ \mu$m and $P = 2d_h$. Images are taken at varying times: (a) 30 s, (b) 130 s, and (c) 190 s after the mask is placed above film. (d) The size of the depleted zone as a function of drying time for masks with $d_h = 250\ \mu$m and $P = 2$ or $5d_h$. (Note: The dashed yellow circles in (a) denote the locations of the holes within the mask.)

To explore the effects of initial colloid volume fraction on pattern formation, we deposit suspensions of varying ϕ_i under a mask of fixed design and obtain optical images and height profiles of the dried, patterned films using a digital camera (S2 IS Canon U.S.A., Inc.) and an optical measuring pen with a 130 μm measurement range (Micro Photonics, Inc.) attached to a computer controlled robotic positioning device (Aerotech, Inc.). We vary ϕ_i from 0.001 to 0.15, fix $d_h = 250\ \mu$m and $P = 2d_h$, and show the optical images as well as the 3D profilometry scans in Figure 3. When ϕ_i is low, the recirculating flows deposit a majority of the particles in the masked regions, leading to inverse pattern formation, as shown in Figure 3a. When ϕ_i is increased, both the width and height of the patterned lines grow. As the volume fraction continues to grow, the particles encroach further

(33) Philipse, A. P.; Vrij, A. *J. Colloid Interface Sci.* **1989**, *128* (1), 121−136.
(34) Verhaegh, N. A. M.; Van Blaaderen, A. *Langmuir* **1994**, *10* (5), 1427−1438.
(35) Bogush, G. H.; Tracy, M. A.; Zukoski, C. F. *J. Non-Cryst. Solids* **1988**, *104* (1), 95−106.

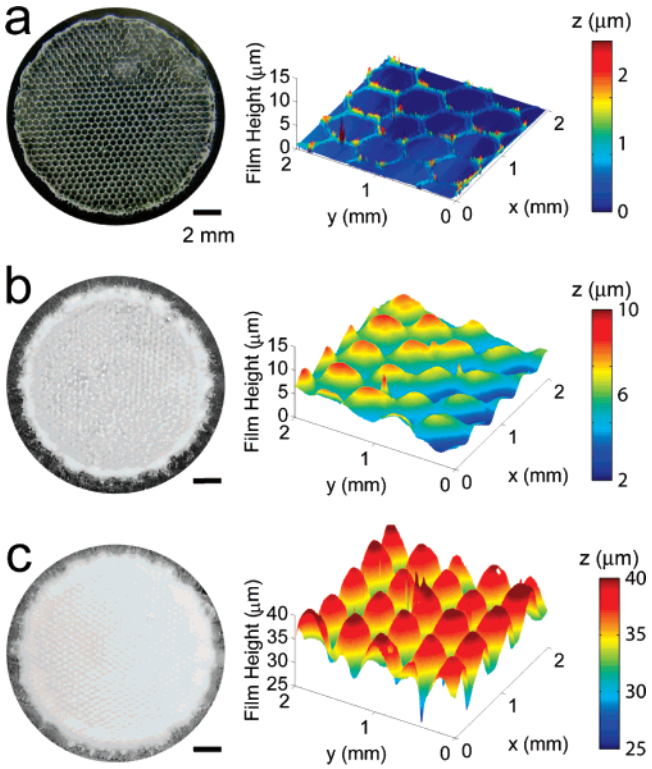

Figure 3. Optical images (left column) and 3D profilometry scans (right column) of colloidal films prepared at varying initial volume fractions: (a) $\phi_i = 0.001$, (b) $\phi_i = 0.05$, and (c) $\phi_i = 0.15$.

into the middle of the unmasked regions, as shown in Figure 3b. When ϕ_i is large ($\phi_i \geq 0.15$), the recirculating flows are quickly suppressed as drying proceeds. At this point, fluid now flows from the masked to the unmasked regions, where the evaporative flux is higher. Concurrently, particle convection occurs, leading to a buildup of particles in the open regions, as shown in Figure 3c. This transition from inverse to normal pattern formation produces films that are analogous to those observed in aqueous colloidal films prepared under similar conditions.[1]

To understand the origin of the observed transition, we prepared a film composed of an initial volume fraction of pure silica microspheres ($\phi_i \approx 0.15$) with a small population of fluorescent-core silica tracers ($\phi_t \approx 5 \times 10^{-6}$). To reduce scattering from the microspheres, the colloids are suspended in an index-matched solvent composed of a 2:3 ratio of ethanol and toluene. Fluorescence images, acquired on a digital camera (Cascade 512B, Roper Scientific, Inc.) attached to an inverted microscope (Axiovert 200M, Carl Zeiss, AG), are shown in Figure 4. The streaks observed in Figure 4a at short times indicate the presence of recirculating flows. The velocities of the fastest particles are calculated by measuring the lengths of the longest streaks and dividing by the exposure time. Typical values for the particle velocity within the recirculating flow cells induced by Marangoni stresses are on the order of 10^{-3} m/s, which is several orders of magnitude larger than the characteristic velocity for purely evaporative flow, $L\dot{E}/h_i \approx 5 \times 10^{-7}$ m/s, where $L = 2.5 \times 10^{-4}$ m is the characteristic size of each recirculating flow cell, $\dot{E} = 2.2 \times 10^{-7}$ m/s is the evaporation rate, and $h_i = 1 \times 10^{-4}$ m is the initial film height. As fluid evaporates and the suspension becomes more concentrated, fewer and shorter streaks are observed in Figure 4b, indicating that the recirculating flows are being increasingly suppressed. Above a critical colloid volume fraction, $\phi_c \approx 0.22$, streaks are no longer observed (Figure 4c), indicating that this flow behavior is now fully suppressed. At the end of the drying process, the contrast increases due to evaporation

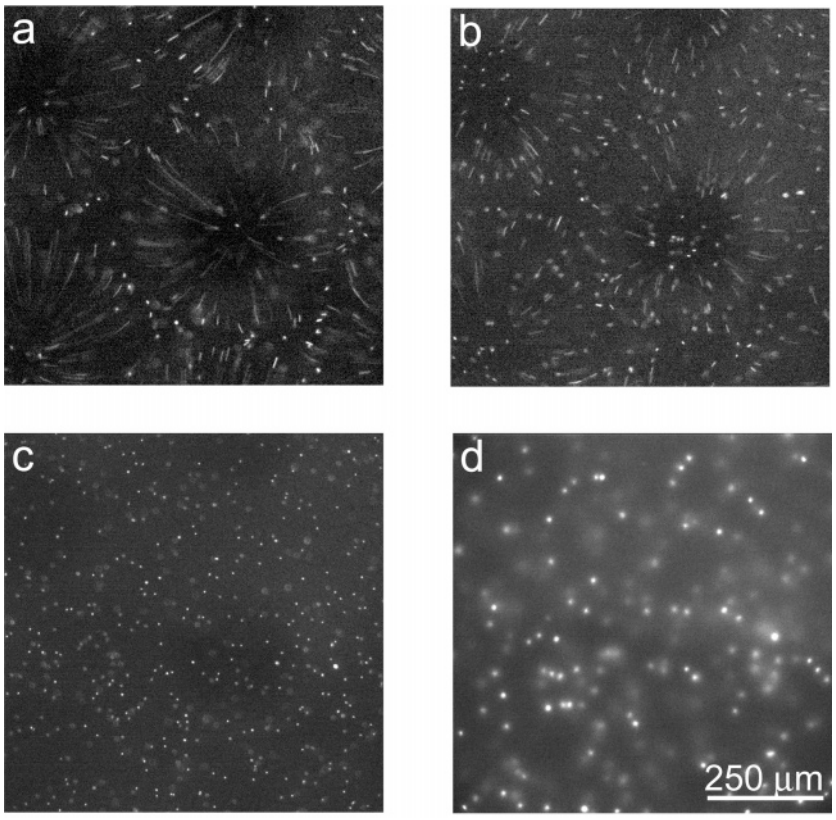

Figure 4. Fluorescence images of the bottom surface of a colloidal film prepared at $\phi_i = 0.15$ and dried under a mask with $d_h = 250$ μm and $P = 2d_h$ at varying evaporation times: (a) 20 s, (b) 35 s, (c) 55 s, and (d) 180 s (dried film). At short times, the streaks in the images indicate fast, recirculating flow. As drying proceeds, the streaks become shorter and ultimately disappear.

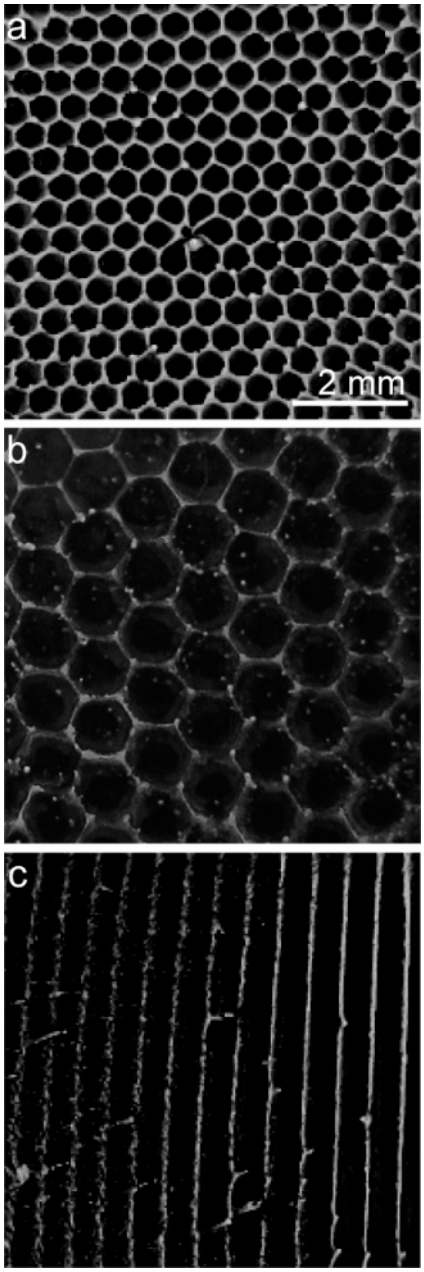

Figure 5. Optical images of colloidal films prepared at $\phi_i = 0.001$ and dried under masks of varying design: (a) an hexagonal array of circular holes, $d_h = 250$ μm and $P = 2d_h$; (b) an hexagonal array of circular holes, $d_h = 500$ μm and $P = 2d_h$; and (c) a parallel array of open lines, $d_l = 200$ μm and $P = 5d_l$.

of the remaining solvent from the film. Hence, the film shown in Figure 4d appears brighter due to particle scattering.

To ensure that cessation of the Marangoni flows is a function of the increased volume fraction and not an unintended consequence of using a co-solvent, a series of colloidal films was prepared with varying ϕ_i and fixed ethanol/toluene ratio, and dried under a patterned mask with $d_h = 250$ μm and $P = 2d_h$. Cessation of the recirculating flows is observed at different times but always at the same $\phi_c \approx 0.22$ for all ϕ_i, suggesting that it is indeed a volume fraction effect (see the Supporting Information). Time-lapsed videos showing the recirculating flows during drying of colloidal suspensions prepared in pure ethanol and pure toluene are provided as Supporting Information.

The size, shape, and arrangement of the recirculating cells are dictated by the design of the drying mask, which controls the evaporation profile and resulting temperature gradient across the film. Evaporative cooling in the unmasked regions creates a film surface that is cooler than the masked, nonevaporating regions. Hence, if the holes in the mask are hexagonally arranged, the film surface will have a hexagonal array of cool regions and recirculating cells. Thus, the final deposited pattern can be easily controlled by modifying the mask design. In films dried under a mask with a hexagonal array of holes with $d_h = 250$ μm and $P = 2d_h$, the Marangoni cells and the resulting particle deposition are hexagonally arranged (Figure 5a) with a spacing of $2d_h$. Doubling the mask hole size and pitch produces films with the same geometric pattern but with larger periodicity (Figure 5b). Drying the films under a mask with parallel open lines produces an array of recirculating cells that yield parallel lines of colloidal particles in the dried film (Figure 5c).

In summary, we have shown that Marangoni-induced recirculating fluid flow leads to remarkable pattern formation during evaporative lithographic patterning of nonaqueous colloidal films. We have demonstrated the ability to produce inverse or regularly patterned colloidal films by varying the initial colloid volume fraction and shown that this transition occurs at a critical volume fraction of 0.22. The temperature gradients across the drop surface, and, thus, the recirculating flows and final film pattern, are easily modified by changing the mask design. Using this novel patterning approach, we have shown that a variety of patterned film geometries can be produced.

Acknowledgment. This material is based on work supported by the U.S. Department of Energy, Division of Materials Sciences under Contract No. DEFG-02-91ER45439, through the Frederick Seitz Materials Research Laboratory. The authors thank H. Hu and J. C. Conrad for useful discussions.

Supporting Information Available: Videos of the recirculating flow cells that develop during evaporative lithographic patterning of colloidal films that consist of fluorescent silica microspheres suspended in pure ethanol and toluene, and fluorescence images of colloidal films prepared with varying ϕ_i and dried under masks of fixed design. This material is available free of charge via the Internet at http://pubs.acs.org.

LA8000637